Modeling and imaging with the generalized screen algorithm

Jérôme H. Le Rousseau and Maarten V. de Hoop

ABSTRACT

Here, we analyze the extension of the phase-screen or split-step Fourier method (Stoffa *et al.*, 1990) to wave propagation in media with large and rapid lateral variations, and including wider scattering angles and back-scattering. The structure of the associated algorithm is similar to the one of the phase-screen algorithm. We demonstrate the accuracy of our algorithm by modeling snapshots and imaging synthetic data in the Marmousi model.

Introduction

In realistic geological models, the heterogeneity in the medium properties is such that the phenomenon of multiple scattering is significant. We distinguish two *classes* of multiple scattering: one where the multiples are identified with respect to the projection of their propagation paths onto the vertical direction (depth), and one where the multiples are identified with respect to the projection of their propagation paths onto the horizontal or lateral plane. In the asymptotic framework of wavefront analysis, paths are rays. The first class of multiple scattering is associated with 'turning rays', the second possibly combined with the first class of multiple scattering, is associated with 'multi-pathing'. A ray-theoretic treatment of these phenomena is not straightforward and is algorithmically rather involved.

A scattering theory that follows the ray picture but accounts for full-wave behavior has been developed by De Hoop (1996). It is based on an extension of the Bremmer coupling series to multi-dimensionally varying media. Bremmer's method decomposes the wave field into a recursion of one-way propagation operators each using the previous wavefield as a source. Thus, the method first generates a wavefield dominated by downward propagation, then generates a 'first' upward propagating wavefield, then a 'second' downward propagating field, etc. In this manner, multiple reflections are accounted for in a controlled manner.

The propagator in the generation of this series is based on a Hamiltonian path-integral representation that accounts for not only the energy travelling along the ray but also for the transport along non-stationary paths. These path integrals reveal any possible multi pathing. The path integral generalizes Gazdag's phase-shift migration operator: the second is valid in laterally homogeneous background media, while the first allows lateral (and vertical) medium variations.

In the path integral, 'time' is identified with depth, and 'momenta' are identified with the horizontal wave slownesses which, in the ray-theoretic limit, coincide with the horizontal components of the gradient of travel time. The (square-root) Hamiltonian is identified with vertical wave slowness which, in the ray-theoretic limit, coincides with the vertical component of the gradient of travel time (De Hoop (1996)).

The problem with the path integrals is the computational complexity of their numerical evaluation. De Hoop *et al.* (1998) have developed a method that reduces the computational complexity of such evaluation dramatically at the cost of adjusting the acoustics (the shape of wave fronts). The result is an algorithm that, per propagation step, is built from a multiplication - forward Fourier transform - multiplication - inverse Fourier transform, where the transform is in the horizontal directions and may be windowed. Since this algorithmic structure coincides with the one of the classical phase-screen propagator, we denote our approximations as generalized screens. We have designed a hierarchy of increasingly accurate approximations. Underlying these approximations is an expansion of the background medium simultaneously into magnitude and smoothness of variation.

The original phase-screen method was designed for multiple downward scattering of waves, the downward direction being the preferred direction of propagation. Thus it included phenomena such as focussing and defocussing. The applicability of the phase-screen method generally requires that the screen interval satisfies the following criteria: small medium variations (weak scat-

tering), laterally smooth medium variations (narrow angle scattering), and even smoother variations in the preferred direction (negligible backscattering). With the generalized screen approach, we access the accuracy of the phase-screen method, and generalize it to larger-contrast, wider-angle, and back-scattering.

Our approach accounts for the *first* class of multiple scattering through the generalized Bremmer series (De Hoop, 1996), and accounts for the *second* class of multi pathing through the generalized screen propagation (De Hoop *et al.*, 1998).

The one-way wave propagator

Let x_3 denote depth. Consider a thin vertical slab, $[x_3', x_3]$, with thickness $\Delta x_3 = x_3 - x_3'$. Denote horizontal or lateral coordinates by x_1 (two-dimensional configuration) or (x_1, x_2) (three-dimensional configuration). We will show the analysis for the two-dimensional configuration.

In the *complex-frequency* (s-) domain, for a vertical step Δx_3 sufficiently small, the Hamiltonian path-integral representation for the one-way wave propagator reduces to (De Hoop, 1996)

$$\hat{g}(x_1, x_3; x_1', x_3') \simeq \int (s/2\pi)^2 \exp[-\mathrm{i}s\,\alpha_1(x_1 - x_1')] \exp[-s\,\hat{\gamma}(x_1, \bar{x}_3, \alpha_1)\,\Delta x_3]\,\mathrm{d}\alpha_1, \tag{1}$$

where

$$\bar{x}_3 = x_3 - \tfrac{1}{2}\Delta x_3. \tag{2}$$

The quantities s and α_1 relate to circular frequency ω and *horizontal wave slowness* p as $s = \mathrm{i}\omega$ and $\alpha_1 = -\mathrm{i}p$. The phase factor in expression (1) contains a symbol $\hat{\gamma}$ related to *vertical wave slowness*, which, in the high-frequency approximation, reduces to (De Hoop *et al.*, 1998)

$$\gamma_1(x_1, \bar{x}_3, \alpha_1) = \sqrt{c^{-2}(x_1, \bar{x}_3) + \alpha_1^2}\,. \tag{3}$$

This approximation, mathematically, represents the principal part of the vertical wave slowness symbol. This principal part corresponds to the vertical component of the gradient of travel time, in accordance with the solution of the eikonal equation. Note that upon multiplying vertical wave slowness by circular frequency we obtain *vertical wave number*: $k_3 = \omega\gamma_1$; *horizontal wave number* is given by $k_1 = \omega p$. With these transformations of variables, in the limit of a laterally homogeneous thin slab, our propagator reduces to Gazdag's phase-shift operator (Gazdag, 1978).

The phase: a symbol expansion

To arrive at a screen-style representation of the one-way wave propagator, we will expand the symbol in Eq.(3). In the thin slab, we introduce a background medium with wavespeed c^0. The background medium is assumed to be constant in the slab, but may vary from one slab to another. We express this by letting $c^0 = c^0(x_3)$. In the background, the vertical slowness is given by

$$\gamma^0(\zeta, \alpha_1) = \sqrt{(c^0)^{-2} + \alpha_1^2} = \gamma^0(x_3, \alpha_1) \text{ if } \zeta \in [x_3', x_3]\,.$$

To avoid that an artificial branch point would enter the propagating-wave domain, we assume that

$$c(x_1, \zeta) \geq c^0(x_3)\,.$$

Now, introduce the contrast function as

$$a_2^1(x_1, \zeta, x_3) = c(x_1, \zeta)^{-2} - (c^0(x_3))^{-2}\,. \tag{4}$$

Then Eq.(3) can be rewritten as

$$\gamma_1 = \sqrt{(\gamma^0)^2 + \mathrm{a}_2^1} = \gamma^0\,\sqrt{1 + \mathrm{a}_2^1/(\gamma^0)^2}\,. \tag{5}$$

Expanding this expression into a Taylor series yields

$$\gamma_1 = \gamma^0 + \gamma_1^1 \tag{6}$$

with

$$\gamma_1^1 = \sum_{I=1}^{n} a_I \frac{(\mathrm{a}_2^1)^I}{(\gamma^0)^{2I-1}} + o((\mathrm{a}_2^1)^n)\,, \tag{7}$$

representing the perturbation in vertical wave slowness. The relevant property of this series expansion is that each term factorizes in x_1 and α_1.

The phase-screen approximation follows from expansion (7) by setting $n = 1$ and approximating $1/\gamma^0$ by its zero-order Taylor expansion in α_1 about 0 (vertical propagation). The split-step Fourier approximation (Stoffa *et al.*, 1990) equals the phase-screen approximation subject to replacing the background wavespeed from *minimum* value to *average* value in the thin slab.

The generalized screen propagator

Substituting Eq.(6) into the propagator in Eq.(1) yields

$$\hat{g}(x_1, x_3; x_1', x_3') \simeq \int (s/2\pi)^2 \exp[-\mathrm{i}s\,\alpha_1(x_1 - x_1')] \exp\{-s\,[\gamma^0(x_3, \alpha_1) + \gamma_1^1(x_1, \bar{x}_3, \alpha_1)]\,\Delta x_3\}\,\mathrm{d}\alpha_1\,. \tag{8}$$

In this representation we extract propagation along vertical according to

$$\gamma_1^1(x_1, \bar{x}_3, \alpha_1) = \gamma_1^1(x_1, \bar{x}_3, 0) + [\gamma_1^1(x_1, \bar{x}_3, \alpha_1) - \gamma_1^1(x_1, \bar{x}_3, 0)] \tag{9}$$

and expand the exponential $\exp\{-s\,[\gamma_1^1(x_1, \bar{x}_3, \alpha_1) - \gamma_1^1(x_1, \bar{x}_3, 0)]\,\Delta x_3\}$ into a Taylor series. Thus

$$\hat{g} \simeq \hat{g}^0 + \hat{g}^1\,, \tag{10}$$

where $\hat{g}^0(x_1, x_3; x_1', x_3')$ has the structure of the split-step Fourier approach,

$$\hat{g}^0(x_1, x_3; x_1', x_3') = \exp[-s\,\gamma_1^1(x_1, \bar{x}_3, 0)\,\Delta x_3]$$

$$\int (s/2\pi)^2 \mathrm{d}\alpha_1 \exp[-\mathrm{i}s\,\alpha_1(x_1 - x_1')] \qquad (11)$$

$$\exp[-s\,\gamma^0(x_3, \alpha_1)\,\Delta x_3]\,,$$

and $\hat{g}^1(x_1, x_3; x_1', x_3')$ represents the generalized screen contribution,

$$\hat{g}^1(x_1, x_3; x_1', x_3') = -s\Delta x_3 \sum_{I=1}^{n} a_I (\mathrm{a}_2^1(x_1, \bar{x}_3, x_3))^I$$

$$\exp[-s\,\gamma_1^1(x_1, \bar{x}_3, 0)\,\Delta x_3]$$

$$\int (s/2\pi)^2 \mathrm{d}\alpha_1 \exp[-\mathrm{i}s\,\alpha_1(x_1 - x_1')] \qquad (12)$$

$$\exp[-s\,\gamma^0(x_3, \alpha_1)\,\Delta x_3]$$

$$\left[\frac{1}{(\gamma^0(x_3, \alpha_1))^{2I-1}} - \frac{1}{(\gamma^0(x_3, 0))^{2I-1}}\right] .$$

The order of the generalized screen approximation is n. The higher the order, the higher the accuracy for wide-angle propagation. The order $n = 1$ propagator simply yields a shuttling between the horizontal space and horizontal slowness domains together with a multiplication in each domain. Each additional term of the generalized screen expansion (7) requires an additional Fourier transform in space. As the *computational complexity* of the downward continuation in the split-step Fourier method is proportional to $2N \log_2 N$, the complexity of our nth order generalized screen approach is proportional to $(2 + n)N \log_2 N$.

The Taylor expansion of the exponential in Eq.(12) destroys the unitarity of the propagator and hence the amplitude characteristics. To restore, approximately, the amplitude behavior we apply a normalization and obtain the generalized screen propagator (GPS)

$$\hat{g}_{\mathrm{GPS}} = \hat{g}^0\,\mathcal{N}\left[1 + \frac{\hat{g}^1}{\hat{g}^0}\right] . \qquad (13)$$

The normalizing operator $\mathcal{N}$ is given by

$$\mathcal{N}[1 + p + \mathrm{i}q] = \exp(\mathrm{i}q)\,\left|1 + \frac{p}{1 + \mathrm{i}q}\right|^{-1}\left[1 + \frac{p}{1 + \mathrm{i}q}\right] ,$$

where p and q are the real and imaginary parts of a complex number. This normalization restores the amplitude behavior exactly for of a constant medium perturbation.

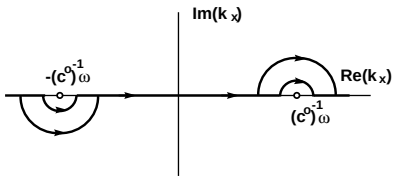

Figure 1. Contour deformation.

The generalized screen algorithm

Here, we discuss the generalized screen algorithm associated with the generalized screen propagation described in Eqs.(8)-(12). We denote the (one-way) wavefield by $\hat{W}$ and we will apply the transformation of variables $(s, \alpha_1) \rightarrow (\omega, k_1)$. Note that each frequency ω can be evaluated independently, so computations can be performed in parallel. The algorithm consists of four steps.

Let the current depth be set to $x_3' = z$. Following Eq.(12), we introduce the intermediate field quantities $w_0, \cdots, w_n$ according to (*step 1*)

$$w_0(x_1) =$$

$$\exp[-\mathrm{i}\omega\Delta x_3\,(c^{-1}(x_1, \bar{x}_3) - (c^0(z))^{-1})]\,\hat{W}(x_1, z, \omega)\,,$$

$$w_I(x_1) = -\mathrm{i}\omega\Delta x_3\,a_I(\mathrm{a}_2^1(x_1, \bar{x}_3, z))^I w_0(x_1)\,,$$

$$I = 1, \cdots, n\,.$$

These intermediate fields quantities are then Fourier transformed to the horizontal-wave-number domain, $w_I(x_1) \rightarrow \tilde{w}_I(k_1)$, $I = 0, \cdots, n$ (*step 2*). The wavefield at depth $x_3 = z + \Delta x_3$ then follows as

$$\tilde{W}(k_1, z + \Delta x_3, \omega) = \tilde{w}_0(k_1)\,\exp[-\mathrm{i}\omega\Delta x_3\,\gamma^0(z, k_1/\omega)]$$
$$\mathcal{N}\left[1 + \frac{\tilde{w}_1(k_1)}{\tilde{w}_0(k_1)}\,\left(\frac{1}{\gamma^0(z, k_1/\omega)} - c^0(z)\right) + \cdots\right. \qquad (14)$$
$$\left. + \frac{\tilde{w}_n(k_1)}{\tilde{w}_0(k_1)}\,\left(\frac{1}{[\gamma^0(z, k_1/\omega)]^{2n-1}} - [c^0(z)]^{2n-1}\right)\right]$$

(*step 3*). Finally, we carry out the inverse Fourier transform, $\tilde{W}(k_1, z + \Delta x_3, \omega) \rightarrow \hat{W}(x_1, z + \Delta x_3, \omega)$ (*step 4*).

Some numerical issues

In Eq.(5), by separating γ^0, we have introduced artificial branch points in the complex α_1-plane, viz. at $\pm(c^0)^{-1}$. These branch points appear also in the expansion (7) for the principal part of the vertical wave slowness symbol, and in expansion (12) for the generalized screen propagator. As a consequence, in Eqs.(11)-(12), the path of integration in the α_1-plane should be chosen appropriately around the branch cuts. In a numerical scheme, in addition, we have to stay far enough away from the artificial branch points to prevent loss of precision: the

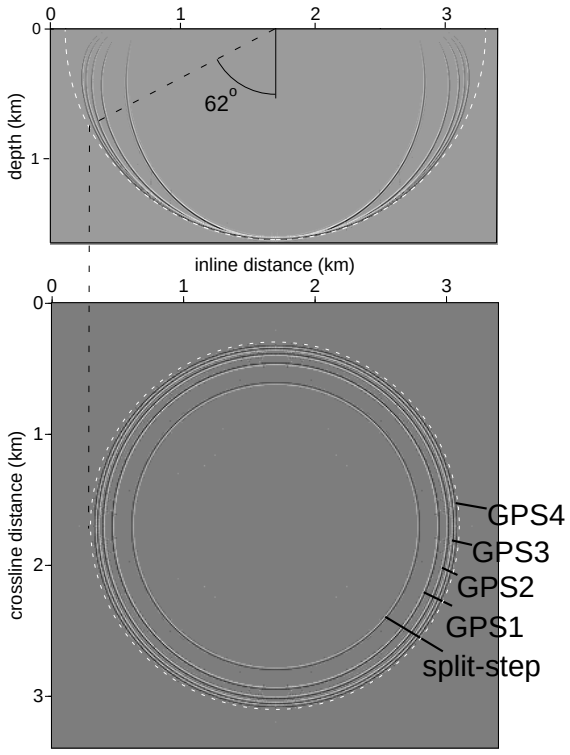

Figure 2. Wavefield snapshots associated with the various generalized screen (1^{st} to 4^{th} order) and the split-step Fourier approximations for a constant medium perturbation.

higher the order n of our generalized screen algorithm, the higher the power in reciprocal background vertical wave slowness, the further we have to stay away from the artificial branch points. (The artificial branch points are associated with propagation in the horizontal directions.) The procedure is illustrated in Fig. 1.

In practice, we apply the contour deformation to all factors appearing in the generalized screen algorithm, except for the intermediate field quantities in the wave number domain. These are assumed to vary smoothly away from the real axis and hence are approximated by their values on the real axis.

Accuracy analysis: modeling

We illustrate the accuracy of our generalized screen algorithm for two cases: a constant medium perturbation, and the Marmousi model. The case of a constant medium perturbation provides us insight in how wave fronts evolve based on Huygens' principle. Let the background medium be characterized by a wavespeed c^0 that is 2/3 of the true wavespeed. We generated impulse responses of the one-way propagator for different orders of generalized screens, as well as for the split-step Fourier

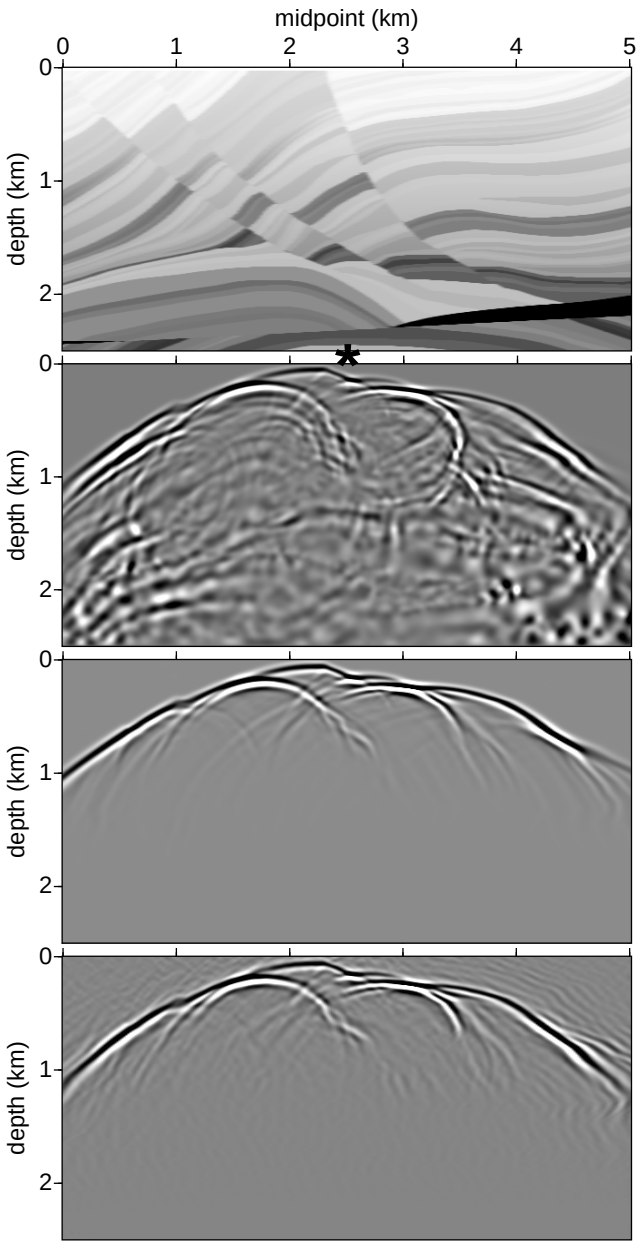

Figure 3. a. Part of the Marmousi model. The asterisk indicates the position of the source. b. Snapshot obtained with the full acoustic wave equation (finite differences). c. Snapshot obtained with the split-step Fourier method. d. Snapshot obtained with the fourth-order generalized screen method. All snapshots at time $t = 0.95$ s.

method. The results are shown in Fig. 2, in which the singular support of the exact response is plotted dashed. Note that the accuracy varies with propagation angle or dip, and that this accuracy *also* varies with (local) medium contrast. In all the approximations, independent of order n, the propagation speed in the horizontal

directions is c^0, which causes any approximate instantaneous wave front to fold inwards away from the true instantaneous wave front. As such, the generalized screen approximation differs, for example, from the paraxial approximation where the accuracy with dip is independent of the medium. From Fig. 2 we conjecture that, as a rule of thumb, the split-step Fourier method is accurate up to 17^o; the first-order generalized screen is accurate up to 34^o, the second-order up to 48^o, the third-order up to 55^o, and the fourth-order up to 62^o. The rate of convergence with order is also apparent in Fig. 2.

The Marmousi model offers a realistic structure with complexities that can be encountered in the real world (Bourgeois *et al.*, 1991). We computed snapshots generated by a point source located at the reservoir horizon, below a complex part of the model (anticline, unconformity, faults). In Fig. 3 the snapshots of the upgoing wavefield are shown for the fourth-order generalized screen algorithm and the split-step Fourier method. Both snapshots are compared with a finite-difference computation of the two-way wavefield. The differences between the snapshots are pronounced only in the secondary arrivals, which are associated with multi pathing and scattering at relatively wide angles. The secondary arrivals constitute key contributions to the imaging of data generated in the Marmousi model.

Application: pre-stack depth migration

We incorporated our generalized screen algorithm in pre-stack depth, shot-gather migration. In Fig. 4 close-ups of images of the Marmousi data are shown. The differences between the images obtained with the split-step Fourier method and the second-order generalized screen algorithm, though subtle, are apparent at the unconformity and the reservoir. In particular, the image of the top of the reservoir obtained with the generalized screen algorithm follows the model grid wise. If the waves in the model would have been scattered at larger angles, the results would have been more pronounced.

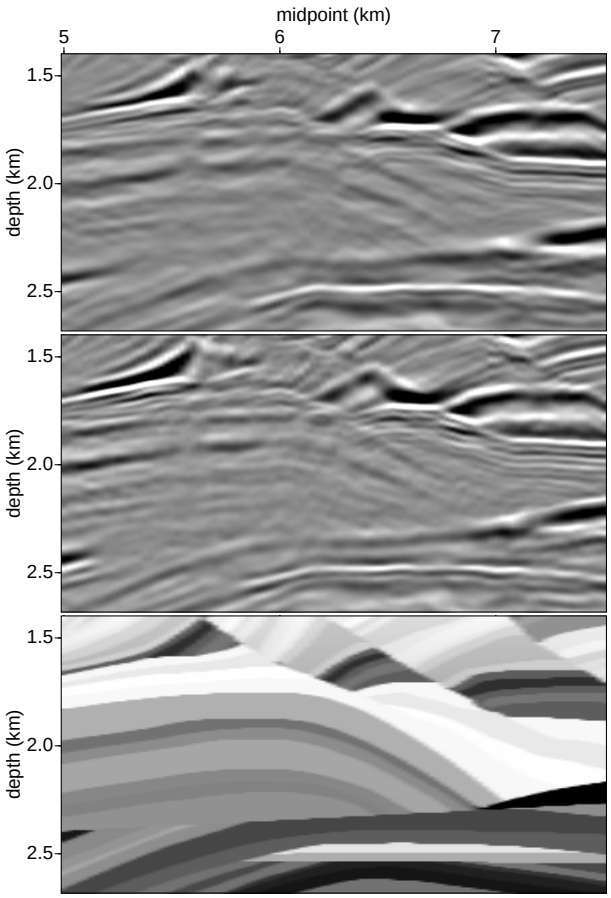

Figure 4. Split-step Fourier image (top); second-order generalized screen image (middle); velocity model (bottom).

Acknowledgments

We would like to thank Edward Jenner for his helpful advice on the numerical implementation. The first author would like to thank Elf Exploration and Production for the support of this research.

References

Bourgeois, A., Bourget, M., Lailly, P., Poulet, M., Ricarte, P., & Versteeg, R. 1991. Marmousi, model and data. *Proc. 1900 EAEG workshop on Practical Aspects of Seismic Data Inversion.*

De Hoop, M. V. 1996. Generalization of the Bremmer coupling series. *J. Math. Phys.*, **37**, pp.3246–3282.

De Hoop, M. V., Wu, R., & Le Rousseau, J. H. 1998. General formulation of screen methods for the scattering of acoustic waves. *in press.*

Gazdag, J. 1978. wave equation migration with the phase-shift method. *Geophysics*, **43**, 1342–1351.

Stoffa, P. L., Fokkema, R. M., de Luna Freire, & Kessinger, W. P. 1990. Split-step Fourier Migration. *Geophysics*, **55**, 410–421.